Vol. 32 (2001) *ACTA PHYSICA POLONICA B* No 6

RESULTS ON *B* DECAYS FROM BaBar *

VASIA SHELKOV

on behalf of the BaBar Collaboration

Lawrence Berkeley National Laboratory, University of California
Berkeley, CA 94720, USA

(Received March 29, 2001)

We present a summary of 1999–2000 BaBar results from BaBar corresponding to about 8–9 fb^{-1} of integrated luminosity. All the numbers given in this writeup are preliminary. We report on measurements of B meson lifetime, $B^0\overline{B}^0$ mixing, sin2β of the CKM triangle, and branching ratios of some charmless B decays.

PACS numbers: 14.40.Nd, 13.25.Hw, 11.30.Er

1. Introduction

In this note we describe some details of experimental analyses and give preliminary results on the following topics:

- the measurements of B lifetimes,
- $B^0\overline{B}^0$ mixing and extraction of of Δm_{B_d},
- overview of sin2β analysis,
- results for charmless decays of B meson.

2. *B* lifetimes

Thanks to the boost of the $\Upsilon(4S)$, the two B mesons produced in BaBar are separated by an average distance in z of ~ 260 μm, and thus the B^0 and charged B lifetimes can be measured.

The first result given here is performed using an inclusive reconstruction of the B^0. An integrated luminosity of 7.9 fb has been used. The B^0 decay

* Presented at the Cracow Epiphany Conference on b Physics and CP Violation, Cracow, Poland, January 5–7, 2001.

which is considered is $\overline{B}^0 \rightarrow D^{*+}\pi_f^-$ where the D^{*+} is signed only by the soft pion coming from the decay $D^{*+} \rightarrow D^0\pi_s^+$. This soft pion is combined with the fast bachelor one (π_f^-). There are enough constraints to reconstruct the D^0 missing mass, assuming that the slow and fast pions are coming from a B^0 decay into $D^*\pi$ [2]. The missing mass is shown in figure 1.

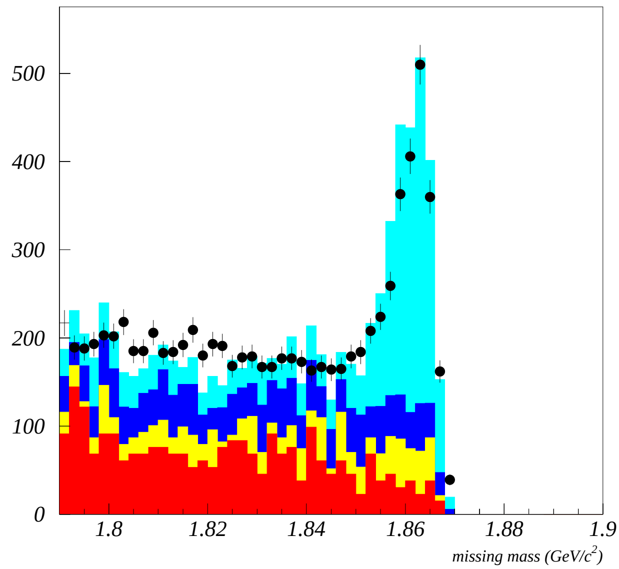

Fig. 1. Missing mass for partially reconstructed $\overline{B}^0 \rightarrow D^{*+}\pi_f^-$ events. The points are the data, the shaded histograms the Monte Carlo contributions.

The B^0 lifetime is measured to be :

$$\tau(B^0) = 1.55 \pm 0.05 \pm 0.07\,\mathrm{ps}\,.$$

The main systematics are due to the backgrounds and the Δz resolution function.

The B^0 and $B^\pm$ lifetimes have been also measured using less abundant but fully exclusive B decay modes [3]. The B mesons are reconstructed using $D^{(*+)}\pi$ $D^{(*+)}\rho$, $D^{(*+)}a_1$ and $J\psi K^*$ decay modes. There is only one background source : the combinatorial background which is estimated from the side-bands of the beam energy substituted mass variable. The two proper time fits are shown in figure 2 and the results for an integrated luminosity of 7.4 fb^{-1} are given in Table I.

These B lifetime measurements are in good agreement with the values from the PDG2000 [4].

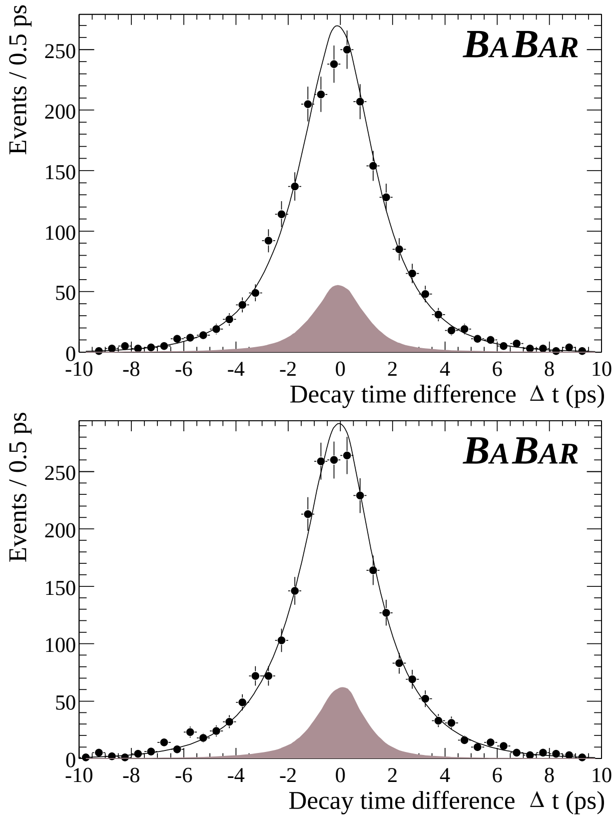

Fig. 2. Δz distributions for the B^0 (right) and charged B (left) candidates. The result of the lifetime fit is superimposed. The background is shown by the hatched distributions.

TABLE I

Measurements of the charged and neutral B mesons lifetimes using fully reconstructed decay modes. The dominant systematics are related to the MC statistics and the background modelling.

$\tau(B^0)$	$1.506 \pm 0.052 \pm 0.029\,\mathrm{ps}$
$\tau(B^\pm)$	$1.602 \pm 0.049 \pm 0.035\,\mathrm{ps}$
$\tau(B^\pm)/\tau(B^0)$	$1.065 \pm 0.044 \pm 0.021$

2.1. Δm_{B_d} measurements

The $\Upsilon(4S)$ resonance decays coherently into a $B^0\,\overline{B}^0$ pair. One of these two B mesons (let us take for example that the B^0) decays at time t_1, then the other one (the $\overline{B}^0$) starts to oscillate and decays at time t_2. If the second B decays as a B^0 the event will be named as *mixed* and the time behaviour will follow a $e^{-|\Delta t|/\tau}(1-\cos\Delta m_{B_d}\Delta t)$ law ($\Delta t = t_1 - t_2$). If it decays as a $\overline{B}^0$ the event is called *unmixed* and the time behaviour will follow a $e^{-|\Delta t|/\tau}(1+\cos\Delta m_{B_d}\Delta t)$ law. The main ingredients for a Δm_{B_d} measurement are:

- to identify the flavour of one B (the one which decays at t_1),
- to tag the flavour of the other B (the one which decays at t_2),
- to measure the distance between the two vertices in order to deduce Δt.

In the first analysis presented here the two B mesons are tagged by two energetic leptons. The performances of the lepton identification are given in Table II.

TABLE II

Efficiencies and misidentification for the lepton used in the dilepton analysis.

Lepton	Efficiency	Misidentification
electron	$\sim 88\%$	$\sim .3\%$
muon	$\sim 75\%$	$\sim 3\%$

The background coming from secondary leptons ($b \to c \to \ell$) is reduced by the use of a Neural Network based on 5 discriminating variables (the two leptons momentum in the $\Upsilon(4S)$ rest frame, the total energy in the event, the missing momentum and the angle between the 2 leptons). The Δm_{B_d} extraction is performed by a binned maximum likelihood fit on the asymmetry between like and unlike sign events. The fit is simultaneously done for Δm_{B_d}, the sample composition (the $\mathrm{B}^{\pm}$ contribution) and the mistag fraction (and its time dependence). The data and the fit are shown in figure 3. With an integrated luminosity of 7.4 fb, Δm_{B_d} is measured to be equal to [5] :

$$\Delta m_{B_d} = (0.507 \pm 0.015 \pm 0.022)\hbar\ \mathrm{ps}^{-1}\,.$$

The Δm_{B_d} measurement using fully reconstructed B^0 is in fact divided into two samples: the hadronic sample with a B^0 reconstructed using $D^{(*)}\pi$, $D^{(*)}\rho$, $D^{(*)}a_1$ and $J\psi\mathrm{K}^*$. With an integrated luminosity of 8.9 fb about 2600

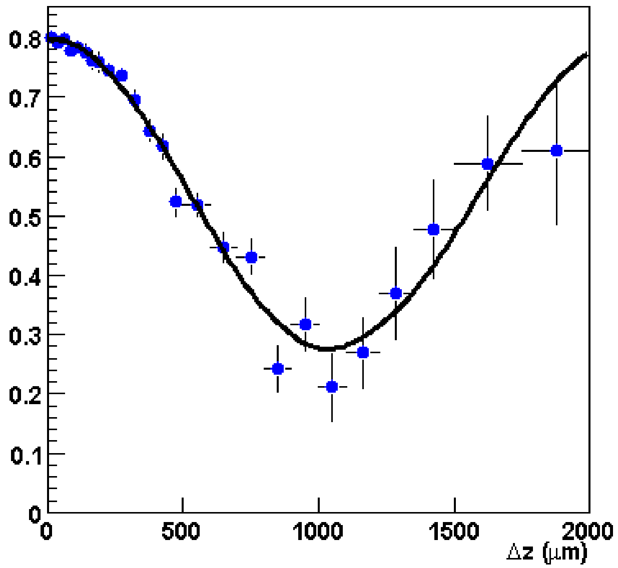

Fig. 3. Distribution of the measured asymmetry between unlike sign (*unmixed*) and like sign (*mixed*) events. Ignoring resolution effects it should follow a $\cos(\Delta m_{B_d}\Delta t)$ law. The curve represents the result of the fit.

candidates with a purity of about 86% are reconstructed. The background is of combinatorial type and is estimated from the side bands of the beam energy substituted mass variable. The other sample is $B^0 \to D^* \ell \bar{\nu}$ which allows to select about 7500 candidates with a purity of roughly 70%.

The flavor of the other B is tagged in the same way as described for $\sin 2\beta$ analysis later in this note.

An unbinned maximum likelihood fit is performed on the probability distribution functions for the *mixed* and *unmixed* events. It treats simultaneously Δm_{B_d}, the main parameters of the resolution function and the mistag fraction. The results are shown below [6]:

$$\begin{aligned} \Delta m_{B_d}\ \text{(had.)} &= (0.516 \pm 0.031 \pm 0.018)\hbar\ \text{ps}^{-1} \\ \Delta m_{B_d}\ \text{(semilep.)} &= (0.508 \pm 0.020 \pm 0.022)\hbar\ \text{ps}^{-1} \end{aligned}$$

The combined result is :

$$\Delta m_{B_d} = (0.512 \pm 0.017 \pm 0.022)\hbar\ \text{ps}^{-1}\,.$$

The main systematics are due to the Δt resolution function, the MC statistics and the $B^\pm \to D^* X \ell \bar{\nu}$ background for the semileptonic sample.

The various Δm_{B_d} measurements are in agreement with the PDG2000 [4].

3. Overview of the sin2β analysis

3.1. Event selection

The sample used for the analysis is 9.8 fb^{-1} of data recorded between January and July 2000 of which 0.8 fb^{-1} was recorded 40 MeV below the $\Upsilon(4S)$ resonance. Particle identification uses mainly the CsI calorimeter for electrons, the Instrumented Flux Return for muons and the DIRC for kaons. Extra information is provided by dE/dx measured in the tracking system. The selection for the CP events proceeds as follows. Pairs of electrons or muons coming from a common vertex are combined to form J/ψ and ψ' candidates. The ψ' is also reconstructed from its decay into $J/\psi\ \pi^+\pi^-$. The K_S candidates are made from either a pair of charged tracks or a pair of π^0 candidates. In addition there are various event shape and topological cuts designed to reduce continuum and $B\overline{B}$ background. Full details of the selection can be found in [10]. The final event sample is shown in figure 4.

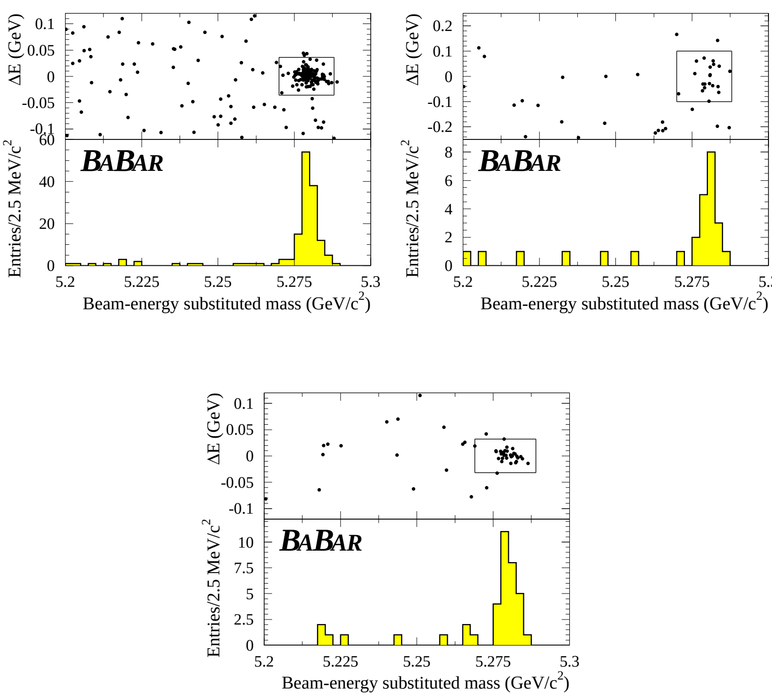

Fig. 4. CP signal event distributions for $J/\psi K_S(\pi^+\pi^-)$ (left), $J/\psi K_S(\pi^0\pi^0)$ (right) and $\psi'\ K_S(\pi^+\pi^-)$ (low).

There are two other B decay samples. One consists of fully reconstructed semileptonic ($B^0 \to D^{*-} l^+ \nu_l$) and hadronic ($B^0 \to D^{(*)-}\pi^+, D^{(*)-}\rho^+, D^{(*)-}a_1^+$) decays as well as a control sample of $B^+ \to \overline{D}^{(*)0}\pi^+$ events. The selection of this sample is described in [11] and [12]. The other is a charmonium control sample containing fully reconstructed neutral or charged B candidates in two-body decay modes with a J/ψ in the final state (*e.g.* $B^+ \to J/\psi\ K^+$, $B^0 \to J/\psi\ K^{*0}(K^{*0} \to K^+\pi^-)$).

3.2. Measuring Δz

The time-dependent decay rate for the B_{CP} is given by

$$f_{\pm}(\Gamma,\, \Delta m_d,\, \mathcal{D}\sin 2\beta,\, t) = \tfrac{1}{4}\Gamma \mathrm{e}^{-\Gamma|t|}\left[1 \pm \mathcal{D}\sin 2\beta\, \sin \Delta m_d t\right]\,, \tag{1}$$

where the + or − sign indicates whether the $B_{\rm tag}$ was tagged as a B^0 or $\overline{B}^0$ respectively. The dilution factor $\mathcal{D}$ is given by $\mathcal{D} = 1 - 2w$, where w is the mistag fraction (the probability that the $B_{\rm tag}$ is identified incorrectly). To account for finite detector resolution, the time distribution must be convoluted with a resolution function:

$$\mathcal{R}(\Delta z;\, \hat{a}) \;=\; \sum_{i=1}^{2} \frac{f_i}{\sigma_i\sqrt{2\pi}}\,\mathrm{e}^{-\frac{(\Delta z-\delta_i)^2}{2\sigma_i^2}}\,, \tag{2}$$

which is just the sum of two Gaussians where the f_i, δ_i and σ_i are the normalisations, biases and widths of the distributions. In practice two scale factors $\mathcal{S}_1$ and $\mathcal{S}_2$ are introduced such that $\sigma_i = \mathcal{S}_i\, \sigma_{\Delta t}$ where $\sigma_{\Delta t}$ is an event-by-event calculated error on Δt. They take account of underestimating the uncertainty on Δt due to effects such as hard scattering and possible underestimation of the amount of material traversed by the particles. The resolution function parameters are obtained from a maximum likelihood fit to the hadronic B^0 sample and are shown in Table III. The f_w parameter represents the width of a third Gaussian component, included to accommodate a small (∼1%) fraction of events which have very large values of Δz, mostly caused by vertex reconstruction problems. This Gaussian is unbiased with a fixed width of 8 ps. Further details can be found in [11].

TABLE III

Resolution function parameters. Those, labeled 'from fit' are measured from data and those marked 'fixed' are determined from Monte Carlo.

Parameter		Value	
δ_1	(ps)	-0.20 ± 0.06	from fit
$\mathcal{S}_1$		1.33 ± 0.14	from fit
f_w	(%)	1.6 ± 0.6	from fit
f_1	(%)	75	fixed
δ_2	(ps)	0	fixed
$\mathcal{S}_2$		2.1	fixed

3.3. B flavour tagging

Each event with a CP candidate is assigned a B^0 or $\overline{B}^0$ tag if it satisfies the criteria for one of the several tagging categories. The figure of merit for each tagging category is the effective tagging efficiency $Q_i = \varepsilon_i (1 - 2w_i)^2$ where ε_i is the fraction of events assigned to category i and w_i is the probability of mis-tagging an event in this category. The statistical error on sin2β is proportional to $1/\sqrt{Q}$ where $Q = \sum_i Q_i$. There are five tagging categories: `Electron, Muon, Kaon, NT1 and NT2`.

The first three require the presence of a fast lepton and/or one or more charged kaons in the event and depend on the correlation between the charge of a primary lepton or kaon and the flavour of the b quark. If an event is not assigned to either the `Electron` or `Muon` categories, it is assigned to the `Kaon` category if the sum of the charges of all the identified kaons in the event is different from zero. If both lepton and kaon tags are available but inconsistent the event is rejected from both categories.

NT1 and NT2 are categories from a neural network algorithm, this approach being motivated by the potential flavour-tagging power carried by non-identified leptons and kaons, correlations between leptons and kaons and more generally the momentum spectrum of charged particles from B meson decays. The output of the neural network tagger $x_{\rm NT}$ can be mapped onto the interval $[-1,1]$ with $x_{\rm NT} < 0$ representing a B^0 tag and $x_{\rm NT} > 0$ a $\overline{B}^0$ tag. Events with $|x_{\rm NT}| > 0.5$ are classified in the `NT1` category and events with $0.2 < |x_{\rm NT}| < 0.5$ in the `NT2` category. Events with $|x_{\rm NT}| < 0.2$ are excluded from the final analysis sample.

3.4. Measurement of tagging performance

The effective tagging efficiencies and mistag fractions for all the categories are measured from data using a maximum likelihood fit to the time distributions of the B^0 hadronic event sample. The procedure uses events which have one B fully reconstructed in a flavour eigenstate mode. The tagging algorithms are then applied to the rest of the event, which represents the potential $B_{\rm tag}$. Events are classified as *mixed* or *unmixed* depending on whether the $B_{\rm tag}$ is tagged with the same or opposite flavour as the B_{CP}. One can express the time-integrated fraction of mixed events χ as a function of the $B^0\overline{B}^0$ mixing probability, $\chi = \chi_d+(1-2\chi_d)w$ where $\chi_d = \frac{1}{2}x_d^2/(1+x_d^2)$, with $x_d = \Delta m_d/\Gamma$. Thus an experimental value of the mistag fraction w can be deduced from the data.

A more accurate estimate of w comes from a time-dependent analysis of the fraction of mixed events. The mixing probability is smallest at low Δt so that this region is governed by the mistag fraction. Figure 5 shows the fraction of mixed events *versus* Δt. The resultant tagging performances are shown in Table IV.

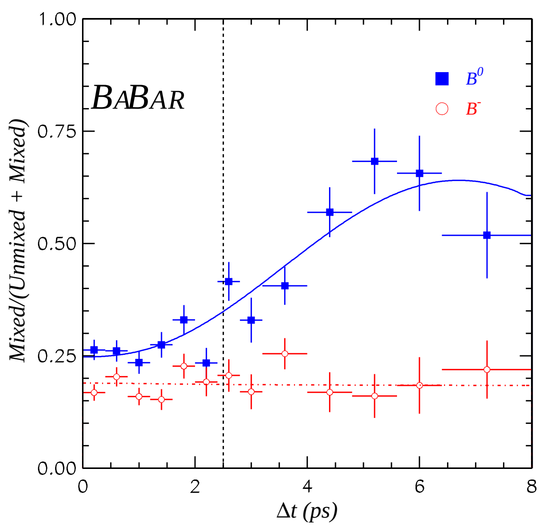

Fig. 5. The fraction of mixed events as a function of $|\Delta t|$ for data events in the hadronic sample for neutral B mesons (full squares) and charged B mesons (open circles). The dot-dashed line at $t_{\rm cut} = 2.5$ ps indicates the bin boundary for the time-integrated single-bin method.

TABLE IV

Tagging performance as measured from data.

Tagging category	ε (%)	w (%)	Q (%)
`Lepton`	11.2 ± 0.5	$9.6 \pm 1.7 \pm 1.3$	7.3 ± 0.3
`Kaon`	36.7 ± 0.9	$19.7 \pm 1.3 \pm 1.1$	13.5 ± 0.3
`NT1`	11.7 ± 0.5	$16.7 \pm 2.2 \pm 2.0$	5.2 ± 0.2
`NT2`	16.6 ± 0.6	$33.1 \pm 2.1 \pm 2.1$	1.9 ± 0.1
all	76.7 ± 0.5		27.9 ± 0.5

3.5. Extracting sin2β

A blind analysis technique was adopted for the extraction of sin2β to eliminate possible experimenter bias. The technique hides both the result of the likelihood fit and the visual CP asymmetry in the Δt distribution. This method allows systematic studies to be performed while keeping the numerical value of sin2β hidden.

Possible systematic effects due to uncertainty in the input parameters to the fit, incomplete knowledge of the time resolution function, uncertainties in the mistag fractions and possible limitations in the analysis procedure were all studied. Details can be found in [10]. The systematic errors are summarised in Table V.

TABLE V

Summary of systematic uncertainties. The different contributions are added in quadrature.

Source of uncertainty	Error on sin2β
uncertainty on τ_B^0	0.002
uncertainty on Δm_d	0.015
uncertainty on Δz resolution for CP sample	0.019
uncertainty on time-resolution bias for CP sample	0.047
uncertainty on measurement of mistag fractions	0.053
different mistag fractions for CP and non-CP samples	0.050
different mistag fractions for B^0 and $\overline{B}^0$	0.005
background in CP sample	0.015
total systematic error	**0.091**

3.6. Results and checks

The maximum likelihood fit for $\sin 2\beta$, using the full tagged sample of 120 $B^0 \to J/\psi K^0_S$ and $B^0 \to \psi' K^0_S$ events yields:

$$\sin 2\beta = 0.12 \pm 0.37\,(\mathrm{stat}) \pm 0.09\,(\mathrm{syst})\ \ (\mathrm{preliminary}). \tag{3}$$

The log likelihood is shown as a function of $\sin 2\beta$ in figure 6. The raw asymmetry as a function of Δt is shown in figure 7

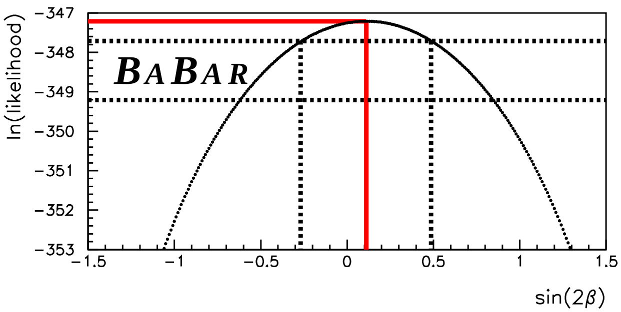

Fig. 6. Variation of the log likelihood as a function of $\sin 2\beta$. The two horizontal dashed lines indicate changes in the log-likelihood corresponding to one and two statistical standard deviations.

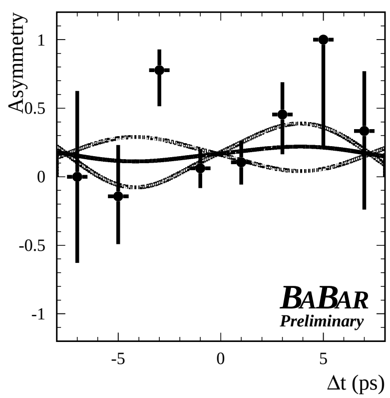

Fig. 7. The raw $B^0 - \overline{B}^0$ asymmetry $(N_{B^0} - N_{\overline{B}^0})/(N_{B^0} + N_{\overline{B}^0})$. The time-dependent asymmetry is represented by a solid curve for the central value of $\sin 2\beta$, and by two dotted curves for the values at plus and minus one statistical standard deviation from the central value. The curves are not centered at (0,0) because the CP sample contains an unequal number of B^0 and $\overline{B}^0$ events (70 B^0 *versus* 50 $\overline{B}^0$). The χ^2 between the binned asymmetry and the result of the maximum likelihood fit is 9.2 for 7 degrees of freedom.

The probability of obtaining a statistical uncertainty of 0.37 is estimated by generating a large number of toy Monte Carlo experiments with the same number of tagged CP events as in the data sample. The errors are distributed around 0.32 with a standard deviation of 0.03, meaning that the probability of obtaining a larger statistical error that the one observed is 5%. From a large number of full Monte Carlo simulated experiments, we estimate that the probability of finding a lower value of the likelihood than the one observed is 20%.

Several cross-checks are performed to validate the main analysis. The charmonium and fully-reconstructed hadronic control samples are composed of events that should exhibit no time-dependent asymmetry. These events are fitted in the same way as the signal CP events to extract an "apparent CP asymmetry". The results are shown in Table VI.

TABLE VI

Summary of systematic uncertainties. The different contributions are added in quadrature.

Sample	Apparent CP asymmetry
Hadronic charged B decays	0.03 ± 0.07
Hadronic neutral B decays	-0.01 ± 0.08
$J/\psi K^+$	0.13 ± 0.14
$J/\psi K^{*0}(K^{*0} \to K^+\pi^-)$	0.49 ± 0.26

4. Results for h^+h^- modes

We select $B^0 \to h^+h^-$ candidates satisfying $5.22 < m_{ES} < 5.3$ GeV/c^2 and $|\Delta E| < 0.420$ GeV. No explicit particle identification is required and the pion mass hypothesis is assumed for both tracks. We require $|\cos\theta_S| < 0.9$ and construct a Fisher discriminant $\mathcal{F}$ from nine variables describing the momentum flow of charged and neutral particles around the B candidate thrust axis.

Signal yields in all three modes are determined simultaneously from an unbinned maximum likelihood fit incorporating m_{ES}, ΔE, $\mathcal{F}$, and the measured θ_c for each track. A sample of D^*-tagged $D^0 \to K^+\pi^-$ decays is used to parameterise the θ_c distributions for pion and kaon tracks as a function of momentum. The K/π separation varies from 2 to 8σ across the relevant momentum range. All candidates in the region $-0.200 < \Delta E < 0.140$ GeV are included in the fit. We find signal yields of $N(\pi\pi) = 29^{+8}_{-7}$, $N(K\pi) = 38^{+9}_{-8}$, and $N(KK) = 7^{+5}_{-4}$. As a cross-check we perform a cut-based analysis requiring a tighter cut on $\cos\theta_{\rm S}$ and additional cuts on $\cos\theta_{\rm B}$ and $\mathcal{F}$. Signal

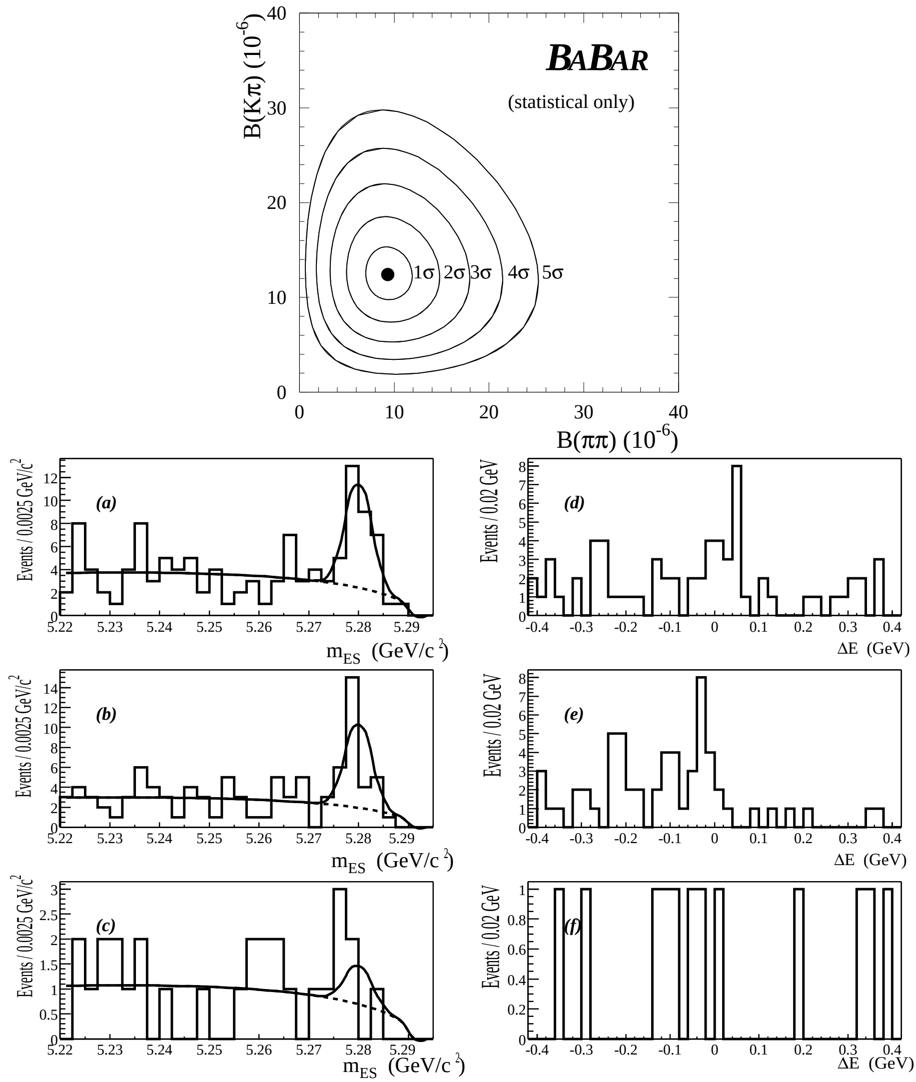

Fig. 8. Upper part: The central value (filled circle) for $\mathcal{B}(B^0 \to \pi^+\pi^-)$ and $\mathcal{B}(B^0 \to K^+\pi^-)$ along with the $n\sigma$ statistical contour curves for the global likelihood fit. Lower part: m_{ES} and ΔE for (a), (d) $\pi\pi$, (b), (e) $K\pi$, and (c), (f) KK candidates in the cut-based analysis.

yields are determined by applying particle identification criteria to isolate independent samples of candidates corresponding to each mode and then fitting the m_{ES} distribution in each sample. The results are consistent with the global likelihood fit. Figure 8 shows the global fit likelihood contour curves for the $\pi\pi$ and $K\pi$ modes, and the m_{ES} and ΔE distributions for the cut-based analysis. The results are summarised in the upper section of Table VII. For the KK mode we calculate the 90% confidence level upper limit. The dominant systematic errors are due to tracking efficiency and the shapes of the ΔE and $\mathcal{F}$ distributions.

TABLE VII

Branching fraction results. Signal yields (N_S) for the h^+h^- modes are determined from a likelihood fit, the rest are obtained by a direct background subtraction. Efficiencies (ε) include intermediate branching fractions.

Mode	N_S	Stat. Sig. (σ)	ε(%)	$\mathcal{B}\,(10^{-6})$
$B^0 \to \pi^+\pi^-$	29^{+8+3}_{-7-4}	5.7	35	$9.3^{+2.6+1.2}_{-2.3-1.4}$
$B^0 \to K^+\pi^-$	38^{+9+3}_{-8-5}	6.7	35	$12.5^{+3.0+1.3}_{-2.6-1.7}$
$B^0 \to K^+K^-$	7^{+5}_{-4} (< 15)	2.1	35	< 6.6
$B^+ \to K^{*0}\pi^+$	10.2 ± 4.8	2.4	10	< 28
$B^+ \to \rho^0 K^+$	10.7 ± 5.1	2.2	10	< 29
$B^+ \to K^+\pi^-\pi^+$	16.3 ± 5.8	3.2	6	< 54
$B^+ \to \rho^0\pi^+$	24.9 ± 8.2	3.3	12	< 39
$B^+ \to \pi^+\pi^-\pi^+$	5.4 ± 5.7	0.7	8	< 22
$B^0 \to \rho^-\pi^+$	35.5 ± 9.8	4.5	8	$49 \pm 13^{+6}_{-5}$
$B^+ \to \eta' K^+$	12.1 ± 3.7	5.3	3	$62 \pm 18 \pm 8$
$B^0 \to \eta' K^0$	1.4 ± 1.4	1.1	0.6	< 112
$B^+ \to \omega h^+$	5.9 ± 3.6	1.7	7.5	< 24
$B^0 \to \omega K^0$	-0.8 ± 0.0	0.0	2	< 14

5. Results for three-body modes

We search for resonant three-body decays by combining a ρ or K^{*0} resonance with a charged pion or kaon. Kaons are required to be positively identified using dE/dx and θ_c information, while tracks not identified as kaons are assumed to be pions. We veto any combination consistent with the decay $D^0 \to K^-\pi^+$. The selection criteria consist of optimised cuts on $\cos\theta_{\mathrm{T}}$, resonance mass, and the angle between the resonance daughters and the B candidate momentum calculated in the rest frame of the vector meson. We also explicitly search for non-resonant $K^+\pi^-\pi^+$ and $\pi^+\pi^-\pi^+$ decays by removing all $K\pi$ and $\pi\pi$ combinations with invariant mass less than $2\,\mathrm{GeV}/c^2$, and all three-body combinations consistent with the decay $B^+ \to J/\psi\, K^+$.

We define a signal region within $6\,\mathrm{MeV}/c^2$ of the B mass in m_{ES} and $\pm 70\,\mathrm{MeV}$ in ΔE. The signal yield is determined by direct background subtraction, where the background in the signal region is estimated from the number of events in the region $5.2 < m_{ES} < 5.27\,\mathrm{GeV}/c^2$. This method is cross-checked using off-resonance data. The results are summarised in the middle section of Table VII. The dominant systematic errors are due to tracking efficiency, π^0 efficiency, and the background subtraction technique.

6. Results for modes with η' or ω

We search for the modes $\eta' K^+$, $\eta' K^0_S$, ωh^+, and ωK^0_S. For $\eta' K$ the kaon is positively identified, while for ωh^+ the charged hadron is assumed to be a pion and the ΔE signal window is increased ($-0.113 < \Delta E < 0.070$ GeV) to take into account the resulting shift in energy when the mass is mis-assigned. The angle between the decay plane of the ω daughters and the B direction in the ω rest frame is used to reduce combinatoric background. We require $|\cos\theta_{\mathrm{T}}| < 0.9$ and optimise with respect to $\mathcal{F}$. Signal yields are determined by background subtraction, where the background is determined from off-resonance data. The results are summarised in the lower third of Table VII. The dominant systematic errors are the same as in the three-body analysis.

7. Conclusions

A preliminary measurements of $B^0\overline{B}^0$ mixing, sin2β and results for some charmless decays by BaBar has been presented.

REFERENCES

[1] G. Sciolla, First results from BaBar, 2000 CP Physics Conference, Ferrara, September 2000.

[2] BaBar Collaboration, SLAC-PUB-8531.

[3] BaBar Collaboration, SLAC-PUB-8529.

[4] D.E. Groom *et al.*, *Eur. Phys. J.* **C15**, 1 (2000).

[5] BaBar Collaboration, SLAC-PUB-8532.

[6] BaBar Collaboration, SLAC-PUB-8530.

[7] BaBar Collaboration, SLAC-PUB-8535.

[8] BaBar Collaboration, Detector Upgrades, `http://www.slac.stanford.edu/BFROOT/www/` Detector/Upgrades/FINALREPORT.pdf

[9] M. Verderi [BABAR Collaboration], `hep-ex/0010076`.

[10] D. G. Hitlin [BABAR Collaboration], in `hep-ex/0011024`.

[11] B. Aubert *et al.* [BABAR Collaboration], decays," `hep-ex/0008052`.

[12] B. Aubert *et al.* [BABAR Collaboration], `hep-ex/0008060`.

[13] P. F. Harrison, H. R. Quinn [BABAR Collaboration], SLAC-R-0504 (section 14 and references therein) Papers from Workshop on Physics at an Asymmetric B Factory (BaBar Collaboration Meeting), Rome, Italy, 11-14 Nov 1996, Princeton, NJ, 17-20 Mar 1997, Orsay, France, 16-19 Jun 1997 and Pasadena, CA, 22-24 September 1997.

[14] BaBar Collaboration, SLAC-PUB-8540.

[15] BaBar Collaboration, SLAC-PUB-8527.

[16] M. Neubert, QCD factorization and CP asymmetries in Hadronic B decays, 2000 CP Physics Conference, Ferrara, September 2000.

[17] BaBar Collaboration, SLAC-PUB-8536.

[18] R. A. Stroynowski, CLEO results on Charmless B meson decays, ICHEP2000, Osaka, July 2000.

[19] P, Chang, Studies of charmless hadronic decays of B mesons with Belle, ICHEP2000, Osaka, July 2000.

[20] BaBar Collaboration, SLAC-PUB-8537.

[21] BaBar Collaboration, SLAC-PUB-8534.